#### **CONFERENCE PRE-PRINT**

## T-15MD: MISSION AND RECENT EXPERIMENTAL RESULTS

I.O. ANASHKIN, E.R. AKHMEDOV, S.V. AKHTYRSKIJ, V.F. ANDREEV, N.A. KIRNEVA, I.I. ARKHIPOV, G.M. ASADULIN, A.YU. BALASHOV, E.E. BARKALOV, K.E. BARKALOV, A.M. BELOV, E.N. BONDARCHUK<sup>(a)</sup>, A.A. BORSCHEGOVSKIJ, V.P. BUDAEV, P.YU. CHISTYAKOV, A.I. CHUDESNOV, A.V. GORBUNOV, A.V. GORSHKOV, S.A. GRASHIN, A.I. GUBANOVA, E.D. DLUGACH, M.M. DREMIN, A.S. DROZD, A.PH. DUBINITSKIJ, L.G. ELISEEV, A.V. EVSEEV, A.D. IZAROVA, YU.V. KAPUSTIN, A.V. KARPOV, N.V. KASYANOVA, R.R. KHAJRUTDINOV, A.V. KHRAMENKOV, A.P. KHVOSTENKO, P.P. KHVOSTENKO, D.A. KISLOV, A.E. KONKOV, P.S. KORENEV, V.A. KRUPIN, A.YU. KUYANOV, I.V. LEVIN, V.E. LUKASH, V.V. LUKYANOV, A.B. MINEEV<sup>(a)</sup>, A.V. LUTCHENKO, A.V. MELNIKOV, D.S. MOLCHANOV, N.A. MUSTAFIN, T.B. MYALTON, K.O. NEDBAJLOV, A.R. NEMETS, S.V. NEUDATCHIN, G.E. NOTKIN, V.N. NOVIKOV, I.S. OBRAZTSOV, A.A. PANASENKOV, D.S. PANFILOV, I.S. PIMENOV, A.S. RZHEVSKIJ, K.A. ROGOZIN, A.N. ROMANNIKOV, I.N. ROY, D.V. RYZHAKOV, D.S. SERGEEV, G.A. SARANCHA, D.V. SARYCHEV, P.V. SAVRUKHIN, D.A. SHELUKHIN, E.A. SHESTAKOV, V.V. SMIRNOV, N.A. SOLOVJEV, A.V. SUSHKOV, D.YU. SYCHUGOV, K.N. TARASYAN, V.I. TEPIKIN, YU.I. TOLPEGINA, D.L. ULASEVICH, V.A. VERSHKOV, I.A. ZEMTSOV

NRC «Kurchatov Institute» Moscow, Russian Federation Email: Kirneva\_NA@nrcki.ru

(a) JSC NIIEFA St. Petersburg, Russian Federation

### **Abstract**

T-15MD is a medium-sized tokamak with R=1.5~m and a=0.67~m. The feature of the device is a low aspect ratio, A=2.2, with an operating range of the toroidal magnetic field up to  $B_T=2~T$ . The physical program of the T-15MD tokamak is focused on the development of quasi-steady state modes with high ion and electron temperature to create an experimental basis of thermonuclear power plants and fusion neutron sources based on tokamak concept. The first plasma in T-15MD was obtained in March 2023. For 2 years, the plasma current up to 0.6 MA were reached, in the range of toroidal magnetic field up to 1.5 T. Plasmas elongation of k>1.5 was reached and the first discharges with divertor configuration were obtained. ECR assisted start-up was used for plasma initiation. The paper presents current status of T-15MD facility, long-term research program and the results of the first experiments.

## 1. INTRODUCTION

Tokamak T-15MD is currently the largest operating tokamak in the Russian Federation. The construction of the device is a development of the fusion researches, which have been carried out at the National Research Center "Kurchatov Institute" for many years [1]. Further development of fusion research and fusion energy in the Russian Federation is associated with two directions: fusion power plant (DEMO) and hybrid fusion-fission systems based on the tokamak as a neutron source (FNS).

The goal of scientific research on tokamak T-15MD is to establish a physical and technological basis for substantiating the development of steady-state FNS of hybrid fusion-fission system based on tokamaks, as well as research activity in support of the International Thermonuclear Experimental Reactor ITER [2].

The first plasma on the T-15MD was obtained on March 31, 2023 [3]. Currently, the tokamak is being brought up to design parameters, and additional heating and diagnostic systems are being put into operation. The features of the T-15MD tokamak, its physical program and the results of the first experiments are described in the paper.

## 2. T-15MD FACILITY

T-15MD is a medium-sized tokamak with R=1.5~m and a=0.67~m [4]. The D-shaped vacuum chamber provides the ability to obtain plasma discharges with an elongation of k up to 1.9 and a triangularity of  $\delta$  up to 0.4. The electromagnetic system of the T-15MD tokamak is designed to obtain a toroidal magnetic field up to  $B_T=2~T$  and plasma current up to  $I_p=2~MA$  in discharge duration up to 10 seconds (for  $B_T=2~T$ ). To obtain long pulse discharges and a high ion and electron plasma temperature, 4 additional heating systems with total power up to 24 MW are under development. In its present day configuration, the T-15MD tokamak is designed to operate on hydrogen. The tokamak first wall and the divertor (open design) are coated by graphite tiles.

Baking and glow discharge in Ar, He and  $H_2$  are used for wall conditioning. Average temperature of vacuum vessel (VV) during the baking is ~110° C with maximal value~140° C and minimal value ~80° C. Vacuum pumping system pipelines are warmed up to  $T = 170 \pm 20^{\circ}$  C [5].

In accordance with the operational range of toroidal magnetic fields and the value of the aspect ratio (A~2.2) the T-15MD tokamak occupies an intermediate position between conventional and spherical tokamaks. This feature will allow the T-15MD to provide additional information required for the development of reactor relevant physical model of tokamak plasmas.

## 2.1. Additional heating and current drive systems of T-15MD tokamak

Four systems of additional heating and current drive are planned for T-15MD tokamak: electron cyclotron heating and current drive (ECRH/ECCD), ion cyclotron heating and current drive (ICRH), low hybrid heating and current drive (LHCD) and neutral beam injection (NBI) [2]. Heating power and current status of these systems is presented in Table 1.

TABLE 1. ADDITIONAL HEATING AND CURRENT DRIVE SYSTEMS OF T-15MD TOKAMAK

System	Expected power, MW	Current status
ECRH/ECCD	8	2 MW gyrotrons are
		under operation
ICRH	6	Design
LHCD	4	Design
NBI	6	Construction

The ECRH/ECCD system by 2030 will consist of 8 MW GYCOM gyrotrons operating with a pulse duration of up to 30 s. Each gyrotron will be equipped with the evacuated transmission line [6]. Launchers are grouped by 4 in 2 equatorial ports and equipped by steerable mirrors to change wave propagation in toroidal ( $\phi_t$  in range of -28° to +21°) and poloidal direction ( $\phi_p$  in range of ( $\mp$ 5°)÷( $\pm$ 30°) in relation to the equatorial plane). The focusing mirrors are installed to get the beam width up to 1.8 cm in the wavebeam constriction. Special transmission lines are developed at the same toroidal cross-sections to provide power launch in the vertical direction. Each launcher will have independent control systems. Currently, 5 gyrotrons have already been delivered to the T-15MD site: 3 tubes have a frequency of f = 82.6 GHz, and 2 gyrotrons have a frequency of f = 105 GHz. Another 3 tubes with f ~ 94 GHz are under development. 2 gyrotrons have been put into operation (1 MW at f = 82.6 GHz and 1 MW at f = 105 GHz). Extraordinary wave on second harmonic of electron cyclotron resonance (ECR) is considered as the main heating mode. However, experiments with plasma heating at the third ECR harmonic can also be carried out in the operating range of the T-15MD toroidal fields [7].

The ICRH and LHCD systems [2] are under engineering design. The ICRH system should provide heating of hydrogen ions at the second harmonic H, minority heating (<sup>3</sup>He and <sup>4</sup>He in hydrogen plasma). Possibility of current drive by fast magnetosonic waves is also considered. To solve the mentioned issues, the frequency range of 15-60 MHz is selected. The total power of the system will be 6 MW with the pulse duration up to 30 s. Two three-loop antennas protected by Faraday screens (3 MW each) will be installed in two toroidal cross-sections.

The LHCD system will consist of 20 klystrons with a frequency of 2.45 GHz, 200 kW each to supply 4 MW of power to the plasma with a pulse duration of 30 s [2]. Power launch will be carried out using a PAM grill.

The NBI system of the T-15MD tokamak consists of 3 hydrogen injectors, each contains of two ion sources. The system provides the ability to operate in quasi-stationary pulse modes with a duration of 30 s (with the possibility of increasing, in the future, to 400 s). Each injector provides oblique launch ( $\phi_t \sim 27^\circ$ ) of hydrogen beam with an energy of up to 60 keV and a total power of up to 2 MW into the T-15MD plasma. Two injectors are currently being installed.

# 2.2. T-15MD diagnostics

T-15MD tokamak diagnostics will be represented by more than 50 systems [2], [8]-[13] that allow measuring the plasma discharge parameters, as well as monitoring the state of technological systems. The set of diagnostics will include traditional systems and innovative ones designed to ensure plasma discharge control and control of facility state (Control), measurement of basic parameters (BP) of plasma and an extended set of characteristics (AP). To ensure the technological cycle of the T-15MD tokamak, systems for monitoring vacuum conditions and temperature of the vacuum chamber and electromagnetic system, monitoring of electrical parameters are provided. Summary on the T-15MD diagnostic systems, measured values and the status of individual systems is presented in Table 2.

TABLE 2. T-15MD DIAGNOSTICS

Diagnostics	Measured parameter	Purpose	Status
Rogowskij coils	$I_p$	Control	Routine operation
Fiber-optics current sensor	$\mathbf{I}_{p}$	Control	Development
Diamagnetic coils	$W_p$ , $\beta_p$	Control	Commissioning
Poloidal Flux coils	$B, U_{loop}$	Control	Routine operation
Two-component magnetic probes	В	Control	Routine operation
Saddle coils	В	AP	Development
Loop voltage sensors	$\mathrm{U}_{\mathrm{loop}}$	Control	Routine operation
Mirnov coils	$\widetilde{\mathrm{B}}$	BP	Commissioning
Fast mobile magnetic probe	$\widetilde{\mathrm{B}}$	AP	Planned
Heavy Ion Beam Probe	B, $n_e$ , $V_p$ , $\varphi$ ,	AP	Development
	and fluctuations		
MSE diagnostic	${ m j}_{ m p}$	BP	Development
High-Res Visible Light Diagnostics	$z_{eff}, T_i, V_p$	AP	Routine operation
Pyroelectric bolometers	$P_{rad}$	BP	Routine operation
AXUV detectors	$P_{\rm rad}$	BP	Routine operation
mm-wave interferometer (1 channel)	$\overline{\mathbf{n}}_{\mathrm{e}}$	Control	Routine operation
Multichannel laser interferometer (LI):			
- heterodyne CO <sub>2</sub> LI	$n_{e}$	BP	Manufacturing
- two-color fiber LI	$n_{\rm e}$	BP	Development
Sweeping (FMCW) reflectometry	$n_{\rm e}$	AP	Development
Correlation reflectometry	$\tilde{\mathrm{n}}_{\mathrm{e}}$ , $\mathrm{V}_{\mathrm{p}}$	AP	Development
Doppler reflectometry	$\tilde{n}_e$ , $V_p$	AP	Development
BES	$\tilde{n}_{e}$	AP	Planned
Helium beam spectroscopy	$n_e, T_e$	AP	Development
Thomson scattering (TS)			•
- tangential view	n <sub>e</sub> , T <sub>e</sub>	BP	Routine operation
- vertical view	n <sub>e</sub> , T <sub>e</sub>	AP	Development
- divertor TS	$n_{e}$	AP	Development
Divertor Lengmuir probes	$n_e$ , $T_e$ , $V_p$ and	BP	Commissioning
	fluctuations		
Fast reciprocating Langmuir probe	$n_e$ , $T_e$ , $V_p$ and	AP	Planned
	fluctuations		
ECE diagnostics	T <sub>e</sub> and fluctuations	BP	Development
Diagnostics of ion temperature fluctuations on the	$T_i$ , $V_p$ and	AP	Planned

heating beam	fluctuations		
Multichannel SXR spectrometer	$T_e, I_{SXR}(E)$	BP	Routine operation (1 ch.)
SXR tomography	$T_e$ , $I_{SXR}$	AP	Routine operation
Visible Light Plasma Emission	$n_{i,n_{z}$	Control	Routine operation
Bremsstrahlung and linear emission	$n_{i,} n_{z}$	BP	Routine operation
Diagnostics of plasma line emission spectra	$n_i, n_z$	Control	Routine operation
CXRS	$T_i$ , $n_i$ , $n_z$ , $V_p$	BP	Commissioning
Laser induced quenching	$T_i$ , $n_i$	AP	Development
Neutral particle analyser	$T_{i}$	BP	Commissioning
X-ray crystalline monochromator	$n_z$	AP	Planned
Fast Ion diagnostics	$V_p$	AP	Planned
SXR monitor	$I_{SXR}$	Control	Routine operation
HXR monitor	$I_{HXR}$	Control	Routine operation
Diagnosis of transient SXR disturbances	$I_{SXR}$ , $\tilde{I}_{SXR}$	AP	Planned
Suprathermal XR tomography	$I_{ST}$	AP	Planned
HXR spectrometer	$I_{HXR}(E)$	Control	Routine operation
n <sup>0</sup> emission monitor	$\mathbf{Y}_{\mathbf{n}}$	Control	Routine operation
n <sup>0</sup> emission tomography	$\mathbf{Y}_{\mathbf{n}}$	AP	Planned
n <sup>0</sup> emission spectrometer	$Y_n(E)$	BP	Planned
Automatic radiation monitoring system	$\mathbf{Y}_{\mathrm{n}},\mathbf{I}_{\mathrm{\gamma}}$	Control	Routine operation
Fast cameras in visible light		Control	Routine operation
Fast cameras in IR light		BP	Planned
Materials Science Station		AP	Planned
Diagnostics of vibrations and deformations of		AP	Planned
tokamak components			
Vacuumetry		Control	Routine operation
Vacuum chamber temperature control		Control	Routine operation
Water cooling monitoring system		Control	Routine operation
Fault indication system		Control	Routine operation
Mass-spectrometry		Control	Routine operation

During the first experimental campaigns the electromagnetic diagnostics were in operation [8]. Thomson scattering diagnostic with tangential probing geometry (TTS) at 10 spatial points [9] and a single-channel X-ray spectrometer were used to measure the electron temperature profile. A single-channel neutral particle analyzer was put into operation to measure the ion temperature. The line average density of plasma was measured using a single-channel microwave interferometer [10], the interferometer signal was used in the density feedback control. The spatial density distribution was determined using TTS diagnostics. The effective plasma charge was obtained from the bremsstrahlung in the visible region using spectroscopic diagnostics. Multichannel X-ray diagnostics, hard X-ray and soft X-ray monitors have been put into operation. Radiation losses were detected by multichannel diagnostics based on pyrodetectors and AXUV detectors. Spectroscopic diagnostics record line spectrum radiation, including  $H_{\beta}$ , CIII, CVI lines, oxygen, nitrogen, helium and other impurity lines. The plasma discharge development was visualized using visible-range video cameras located in two toroidal cross sections. An additional video camera was used to control the state of the ECRH launcher.

Hydrogen is the working gas for the T-15MD plasma. However, in the case of the generation of a runaway electron beam and its interaction with plasma facing components (PFC), the appearance of neutrons due to  $(\gamma, n^0)$  reactions can be observed. Neutron monitors, a neutron spectrometer and an automated radiation monitoring system are used to register neutrons and their spectrum.

Monitoring of engineering parameters, including the pressure in the vacuum chamber and the composition of the residual gas [5], the temperature of the vacuum chamber and the electromagnetic system, the parameters of the winding cooling system, is carried out in real time.

## 3. RESEARCH PROGRAM OF T-15MD TOKAMAK

The research program of the T-15MD tokamak includes scientific (physical and engineering) and organizational tasks. The solution to organizational problems is aimed at developing a scientific school in plasma physics and controlled fusion, expanding the research team, creating an infrastructure to provide the operation of the tokamak and all systems, and developing algorithms for personnel interaction to ensure the life cycle of the facility.

The main objective of scientific research at the T-15MD tokamak is to achieve a quasi-steady state, stable, improved confinement regime in discharges of long-duration (several seconds or more) using additional heating and current drive systems to prepare scenarios for the next-step facilities. Development of high confinement regime requires the development of methods for control of plasma confinement in the peripheral region and in the core. Currently, the H-mode with edge localized modes (ELMs) is considered as the basic regime for the next step tokamaks. Estimations of expected threshold power for L-H transition using scaling laws [14]-[16] show that the transition to the H-mode in the T-15MD hydrogen plasma is possible even with a moderate heating power,  $P_{heat} \sim 3$  MW. The physics research program at the T-15MD tokamak involves studying the mechanisms of L-H transition, as well as exploring the possibility of creating the improved confinement modes with impurity seeding (RI - mode), internal transport barriers (ITB) in scenario with the plasma current profile control, and optimization of the confinement mode with changing of plasma shape. Fundamental problems of tokamak plasma physics will be explored in all the regimes under consideration: mechanisms of energy and particle transport, physical basis of the heating and current drive methods, and mechanisms of instability development.

Achievement and investigation of high- $\beta_p$  modes and regimes with partial or completely non-inductive current maintenance are important to obtain reactor relevant scenario. Algorithms of stability control will be developed including the algorithms of disruption prevention, sawtooth control, control of tearing and neoclassical tearing modes. ELMs etc.

Development of long-pulse discharge technologies involves experiments aimed on the optimization of the plasma-wall interaction. Plasma transport processes in the SOL and divertor region, assessment of heat load distribution on the first wall, and plasma interaction with first wall materials will be studied in various confinement modes. Different methods of wall conditioning will be analyzed, including boronization and lithiation. Divertor physics will be studied including detachment, the effects of gas injection (nitrogen, neon) on the detachment and thermal load distribution in the divertor, testing of active divertor cooling systems in steady-state tokamak operation, and the influence of divertor materials (carbon, tungsten, lithium) on divertor operation and the influx of impurities into the main plasma. Due to the high total power of the additional heating systems, testing of candidate materials and cooled structures of the first wall thermal protection and divertor thermal protection can be carried out in the future with high thermal loads (quasi-stationary > 10 MW/m² and extremely high peak loads during transient processes).

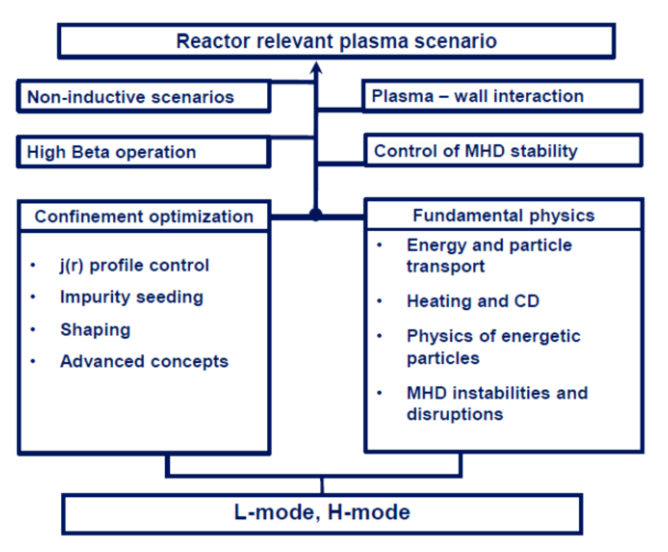


FIG. 1. Framework of the physical research program for the T-15MD tokamak

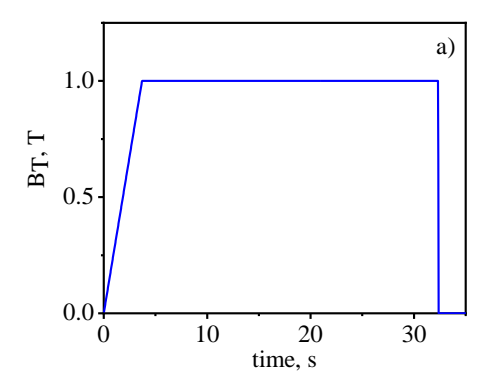
The proposed range of T-15MD researches is shown schematically in Fig. 1

In addition to the objectives outlined above, the experimental investigations at the T-15MD tokamak will address challenges related to the development and testing of technologies required for the future tokamak reactor or FNS. Although the T-15MD has limitations in handling hydrogen isotopes, which precludes the possibility of generating intense neutron fluxes, some technological aspects can be developed even with these limitations. A unique feature of the T-15MD tokamak is the vacuum chamber design with large equatorial ports located close to the plasma. This facilitates plasma diagnostics and will allow for the installation and testing of reactor system mockups (first wall elements and blanket module prototypes) under thermal and electromagnetic loads relevant to real experimental conditions, as well as the development of remote maintenance methods.

#### 4. FIRST EXPERIMENTAL RESULTS

Electromagnetic system of T-15MD tokamak was tested during the first experimental campaign at toroidal field values up to  $B_T = 1.64$  T [3]. The ability to maintain a toroidal field of  $B_T = 1$  T for 30 seconds was demonstrated (Fig. 2, a).

In the first experiments [3] a gyrotron with a frequency of f=82.6 GHz and an output power of 1 MW [6] was used for EC preionization. Taking into account the length of the waveguide path and the presence of turning elements, the power supplied to the plasma was  $P_{EC} \ge 0.85$  MW. An extraordinary polarized wave (X-mode) was used. Breakdown was achieved at a residual pressure of  $p_{bd} \sim (3-5)\ 10^{-5}$  Torr. Experiments were carried out in a limiter configuration with an installed graphite rail limiter with  $a_{lim}=0.67$  m. The surface of the vacuum chamber (stainless steel) in these experiments was not covered with graphite tiles. To obtain a breakdown, the toroidal magnetic field varied from shot to shot in the range  $B_T=0.5-1.2$  T. Due to the small aspect ratio of T-15MD, the resonance regions at the second and third harmonics of the electron cyclotron frequency (ECF) are simultaneously present inside the tokamak vacuum vessel at  $B_T \ge 0.75$  T. It was shown [3] that a breakdown occurs if the resonance layer at the second harmonic of the ECF ( $2\omega_{ce}$ ) is present inside of the vacuum vessel; the breakdown region corresponds to the position of the  $2\omega_{ce}$  resonance (Fig. 2,b).



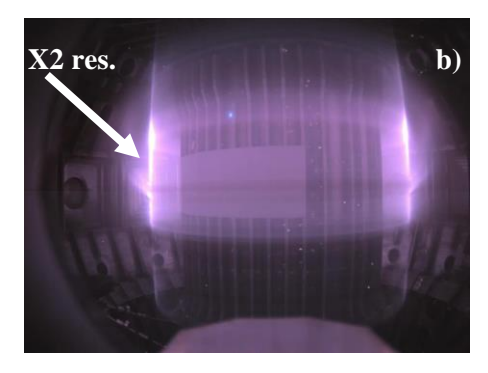
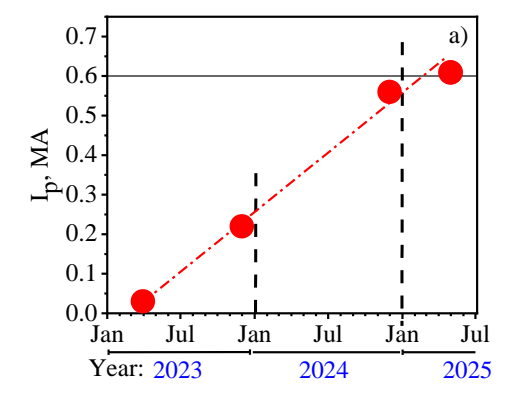


FIG. 2. Results of the first experimental campaign on the T-15MD tokamak: a) the result of testing the toroidal field coils in shot #348; b) obtaining the first plasma - the breakdown region corresponds to the  $2\omega_{ce}$  resonance.

During the first year of operation, the plasma current was increased from 30 to 250 kA (Fig. 3, a). Then the rail limiter was removed, and the first wall of the vacuum chamber was partially covered with graphite tiles (the central column, the lower divertor area, and partially the upper divertor area). Increase of the plasma current required an improvement of the control of the vertical and horizontal plasma position, which was achieved using the results of the numerical analysis discussed below. In the 2024 experiments, the T-15MD facility achieved current values of  $I_p \ge 0.5$  MA (Fig. 3, a), and discharges with an elongation  $k \ge 1.5$  were obtained (Fig. 3, b).



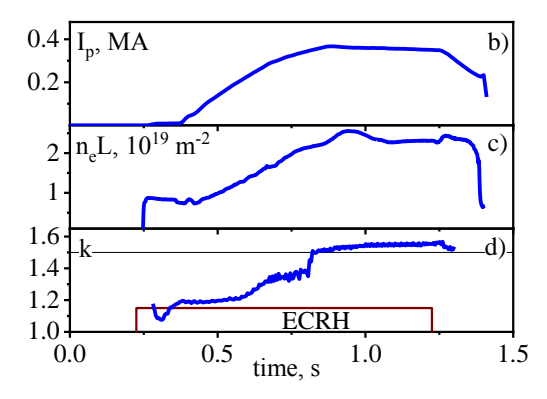
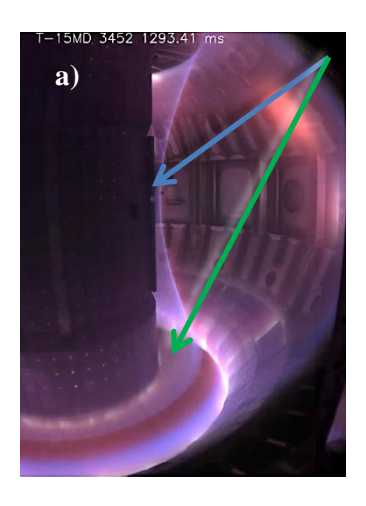


FIG. 3. Increasing the plasma current in experimental campaigns on the T-15MD tokamak (a) and traces of typical shot with an elongated configuration, shot #3166: (b) – plasma current, (c) – chord average density, (d) – plasma elongation.

The development of algorithms for controlling the position and shape of the plasma column made it possible to obtain the first discharges with a divertor configuration (Fig. 4) in plasmas with  $I_p \ge 0.38$  MA and  $k \ge 1.5$ . The transition to a divertor configuration in the T-15MD tokamak is detected by a high-speed video camera, AXUV, bolometers, and Langmuir probes. The X-point formation is confirmed by equilibrium restoration using the FCDI algorithm [17] and the dBound code [18].



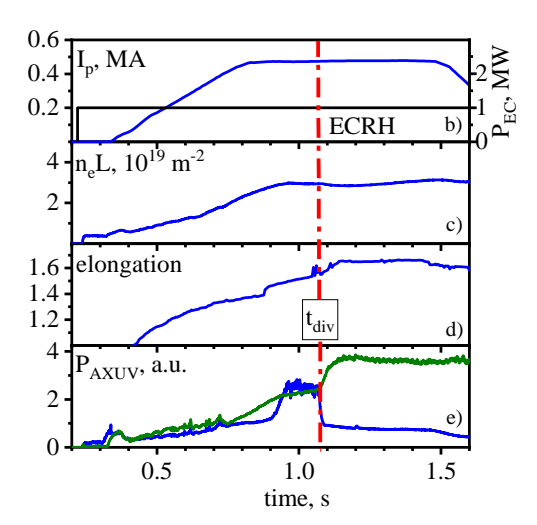
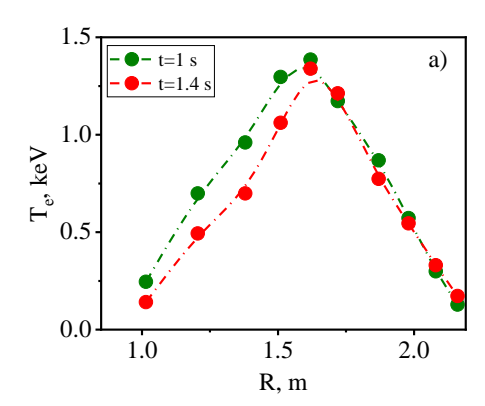


FIG. 4. Shot #3452. Visible light image of the plasma cross section with the formed divertor configuration, t = 1293 ms (a), traces of the plasma current (b), the chord average density  $n_eL$  (c), the plasma elongation (d) and the radiation loss power measured using AXUV detectors along two chords (shown by arrows in Fig. (a)). The instant of the divertor configuration formation  $t_{div}$  is shown in Fig. 4(b)-(d) by the vertical dotted line.

## 4.1. Confinement analysis

Electron temperature and density profiles were obtained from TTS diagnostics (Fig. 5). Analysis of the measured profiles show that in all the obtained modes, both with the divertor and limiter configurations, the plasma in T-15MD is kept in the L-mode – the electron temperature and density profiles remain flat near the separatrix.

As far as the T-15MD tokamak occupies an intermediate position between conventional and spherical tokamaks due to its small aspect ratio but relatively high magnetic field, it is of interest to compare the achieved energy confinement times with the corresponding scaling law. Three pulses with a plasma current of  $I_p \sim 500~kA$ , limiter and diverter plasma configurations, and different elongations were selected for comparison (Table 3).



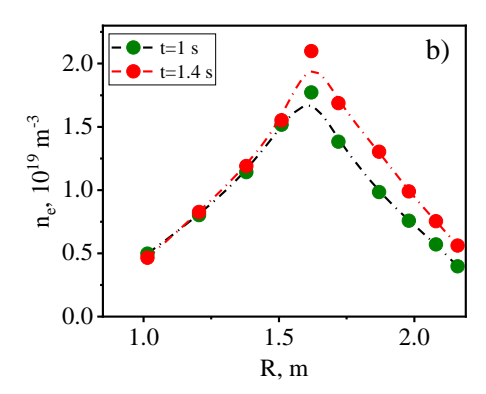


FIG. 5. Shot #3452. Electron temperature (a) and density (b) profiles during limiter phase (t=1 s) and in the divertor configuration (t=1.4 s).

The energy confinement time was calculated as  $\tau_E=W_e/(P_{OH}+P_{EC})$ . Here  $W_e$  – electron energy content obtained from TTS measurements. In all the discharges considered, additional heating of the plasma was carried out using ECRH, and the line average plasma density did not exceed  $\overline{n}_e \leq 2.5 \cdot 10^{19} \text{ m}^{-3}$ , the transport in the ion component was close to the neoclassical one, and the contribution of the ion component to the energy content of

the plasma did not exceed 20%. ITER-89P scaling [19] was chosen for comparison with traditional tokamaks. Multi-machine scaling,  $\tau_{E-ST}$ , proposed in [20] was chosen for comparison with spherical tokamaks. As far as the scaling  $\tau_{E-ST}$  was made for discharges with the H-mode, the energy confinement time determined for T-15MD in the L-mode was compared with the value of  $(\tau_{E-ST})/2$ . The absorbed EC power value was determined using the OGRAY code [21]. Calculations showed that at the quasi-steady state phase of the discharge (at the current plateau), a high fraction (>75%) of single-pass absorption can be expected. At the same time the absorption at  $3\omega_{ce}$  layer can play a significant role (from 10% to 30% of the absorbed power) in discharges with off-axis ECR heating shifted to the high field side due to the low aspect ratio of T-15MD tokamak (Fig. 6).

Better agreement was found (Table 3) between the T-15MD experimental results and the ITER L-89P scaling than with the spherical tokamak scaling. This is likely due to the stronger dependence on R in the  $\tau_{E-ST}$  ( $\tau_{E-ST} \sim R^{2.66}$ ) compared to  $\tau_{E} \sim R^{1.2}$  in the ITER L-89P scaling.

TABLE 3. ACHIEVED ENERGY CONFINEMENT TIME VERSUS SCALING PREDICTIONS

Shot No.	I <sub>p</sub> , kA	k	Configuration	$\tau_{E}$ ,	τ <sub>E-89P</sub> ,	$(\tau_{\text{E-ST}})/2$ ,
				ms	ms	ms
3089	520	1.2	limiter	26	30	110
3166	350	1.55	limiter	30	31	160
3452	470	1.5	limiter	35	36	180
3452	470	1.65	divertor	39	40	185

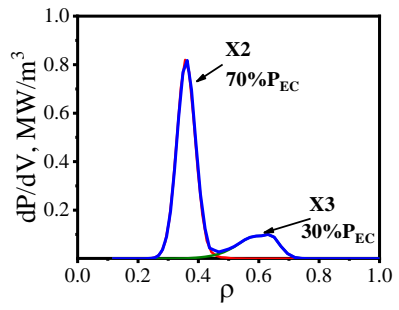


FIG. 6. Absorbed power profile determined using the OGRAY code for shot #3089 (100% single-pass absorption). The fractions of power absorbed at  $2\omega_{ce}$  and  $3\omega_{ce}$  are shown in the plot.

Despite the predominantly off-axis EC power absorption (Fig. 6), sawtooth oscillations were observed during the steady-state phase of the discharge on the microwave interferometer signals and on multichannel SXR diagnostics. The observation of sawtooth density oscillations made it possible to analyze the particle transport in the central part of the plasma column using the method described in [22]. Estimations show that in the discharges studied, the increase in density within the phase reversal radius ( $\rho < \rho_s$ ) in the process between the internal disruptions is satisfactorily described by the neoclassical particle pinch velocity,  $V_p^{\ neo}$ .

## 4.2. Numerical analysis of plasma stability

The increase in plasma current in the first experiments was obtained by using of numerical codes PLASMALESS, TOKSCEN and TOKSTAB to the development of algorithms for controlling the position of the plasma column vertically and horizontally and creating stable magnetic configurations [23].

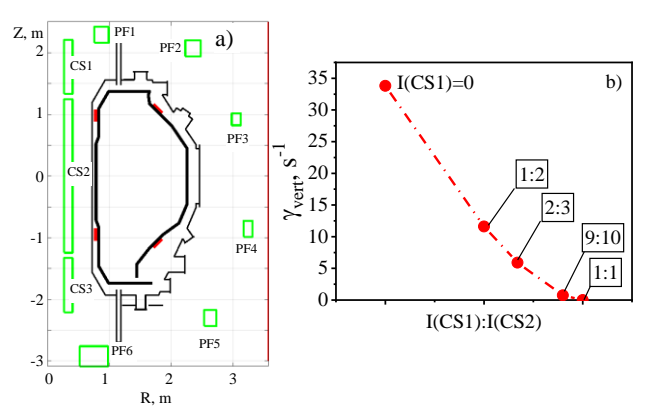


FIG. 7. Layout of the T-15MD electromagnetic system (a) and the TOKSTAB calculation results - the increment of vertical plasma instability as a function of the current ratio in the CS sections (b). The red segments in plot (a) indicate the location of the passive stabilization coils.

Figure 7,a shows the vacuum chamber and the electromagnetic system of the T-15MD tokamak. The central solenoid (CS) consists of three sections, labeled CS1-CS3. Control coils PF1-PF6 are used for creation of the required magnetic configuration and control the plasma position.

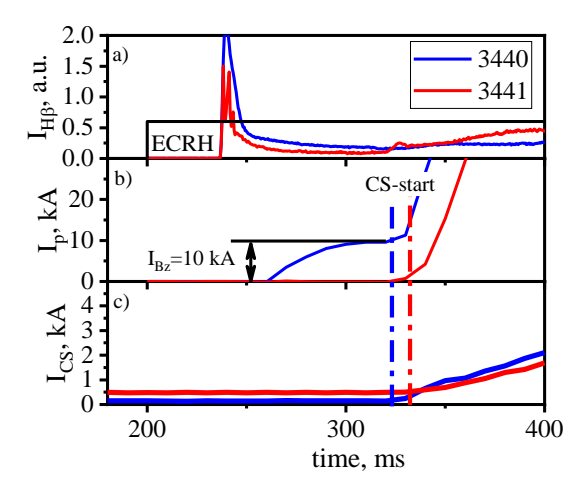
A starting equilibrium was determined using numerical modeling [23] that ensured the stability of the plasma column vertically at low plasma currents ( $I_p\sim10\,$  kA), then a calculation was made of the sequence of stationary equilibria with increasing plasma current. The main trends in the change in increments of the vertical instability with changes in the currents in the solenoid and

control coils were determined. Figure 7,b shows the change in the increment of the vertical stability of the plasma column as a result of an increase in the ratio of I(CS1)/I(CS2) under the condition I(CS1)=I(CS3) and constant currents in the control coils. Based on the simulation, it was shown that relation (I(PF2)+I(PF5))/(I(PF3)+I(PF4))>2 should be satisfied throughout the discharge duration to ensure vertical plasma stability (here I(PF2)-I(PF5) are the currents in the corresponding control coils and I(CS1)-I(CS3) currents in the corresponding parts of central solenoid). Simultaneous changes in the currents in the solenoid sections and currents in the coils PF2-PF5 made it possible to regulate the horizontal position of the plasma column. According to numerical simulations, increasing the solenoid current by 10% while simultaneous proportional decreasing the currents in coils PF2-PF5 results in a plasma column shift toward the low field side by approximately 5 cm. A sensitivity analysis of the numerical simulation results to the plasma column position and the internal inductance  $I_i$  revealed that  $I_i$  changes in the range of  $I_i$ =0.8-1.5 (from flat to a peaked plasma current distribution) has little effect on the current ratio requirements. The resulting ratios were used in the plasma position feedback control, which led to the increase of the plasma discharge duration and achievable plasma current values (Fig. 2,a).

#### 4.3. Non-inductive plasma start-up

The T-15MD discharges were initiated by  $2\omega_{ce}$  EC preionization. Depending on the toroidal magnetic field value, a gyrotron with a frequency either 82.6 GHz or 105 GHz was used. The experiments were carried out in EC power range from 470 kW to 1 MW. The initial working gas pressure in the experiments varied from  $5x10^{-6}$  Torr to  $5x10^{-4}$  Torr. Plasma column formation was observed in the range of  $p_{init} = (5x10^{-6} - 5x10^{-5})$  Torr. At higher  $p_{init}$  values, gas ionization by the microwave wave was observed, but the discharge did not develop in the range of loop voltages up to 6 V.

Two typical T-15MD discharges are shown in Fig. 8a-c. The gyrotron was turned on before the start of the vortex fields, at t = 200 ms, the feedback-controlled buildup of the vortex field (current growth in CS) began after ~130 ms. Microwave breakdown occurred ~30-40 ms after the gyrotron was turned on. Using currents in poloidal windings PF2-PF5, an initial magnetic configuration was created. In this configuration, charge separation due to Bxgrad(B) drift can lead to the formation of a toroidal current even before the vortex fields are activated. The magnitude of this current depends on the initial pressure, the initial magnetic configuration, and the magnitude of the vertical component of the poloidal magnetic field,  $B_z$ . The magnetic configuration corresponding to t = 200 ms in shot 3440 is shown in Fig. 8,d. In shot #3440,  $B_z \sim 45$  Gs in the breakdown region, and the initial toroidal current was  $I_{Bz} = 10$  kA. In shot 3441,  $B_z \sim 15$  Gs in the breakdown region, and no initial current was formed. Experiments showed that the appearance of this current apparently did not depend on the toroidal angle of EC power launch  $\phi_t$ : the effect was observed at both  $\phi_t = 0^\circ$  and  $\phi_t = 18^\circ$ . By optimizing the magnetic configuration, EC breakdown with subsequent  $I_{Bz}$  formation was achieved over the studied range of gyrotron output power values,  $P_{EC} = 0.47 - 1$  MW. The role of the  $I_{Bz}$  current in the development of the discharge and its dependencies on the magnetic configuration parameters, initial gas pressure, EC power, etc. are under investigation.



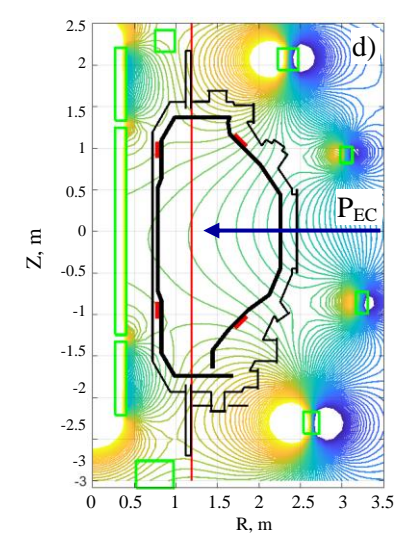
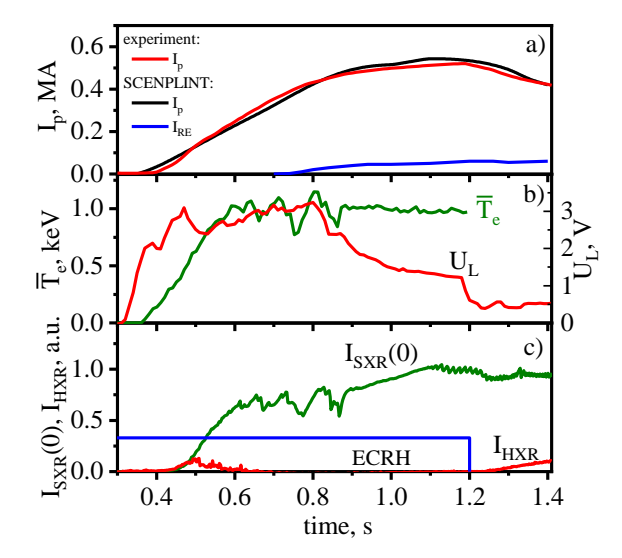


FIG. 8. Initial phase of the discharge. Shots #3440 and #3441: traces of the  $H_{\beta}$  emission (a), plasma current (b), current in the CS2 section of solenoid (c), initial magnetic configuration in shot #3440 prior the start of the vortex fields (d). Position of  $2\omega_{ce}$  resonance layer is shown by vertical red line on Fig. 8,d.

In T-15MD discharges with EC assisted start-up and current ramp-up rise up to  $dI_p/dt \sim 1$  MA/s, the loop voltage did not exceed  $U_L \sim 3.5$  V, hence the longitudinal electric field magnitude  $E_\parallel < 0.35$  V/m during the shot. In shots #3440 and #3441 given above,  $E_\parallel < 0.3$  V/m with  $dI_p/dt \sim 1$  MA/s.

First analysis of the burn-through phase and discharge development was performed using the 0-D code SCENPLINT [24] for shot #3089. Evolution of loop voltage, average electron temperature and average electron density, geometric parameters of the discharge, initial pressure, power and duration of EC heating were used as input data for the SCENPLINT modeling. As a result, the evolution of the plasma current and the current carried by runaway electrons were estimated. Results of the modelling are shown in Fig. 9 in comparison with the experimental data. Simulation predicts the absence of the runaway electrons (RE) up to t~750 ms. Transient decrease of the plasma temperature at t~750 ms (Fig. 9,b) leads to the appearance of the RE beam in simulations (Fig. 9,a). Temperature decrease can be caused by the development of MHD activity during the plasma current ramp-up. According to these simulations possible RE current is small (Fig. 9,a); the plasma current is carried by thermal plasmas. This is consistent with the experimental data which show that all discharges presented in the paper are far from the operational limits in density (Fig. 10).



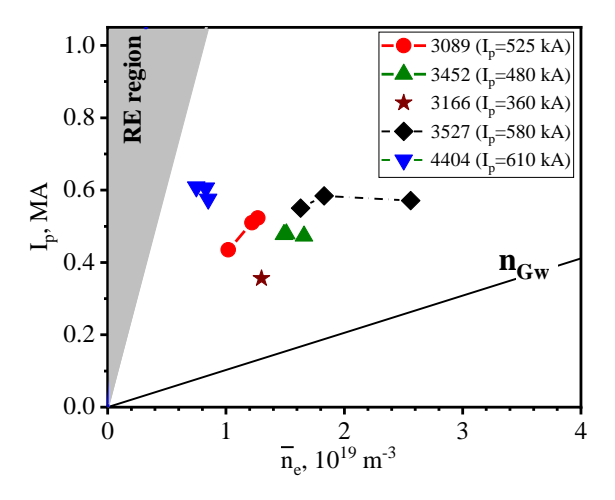


FIG. 9. Shot #3089: (a) plasma current from experimental data, plasma current and RE current from SCENPLINT modeling (a); trace of the average electron temperature from TTS and loop voltage behavior (b); intensity of a soft X-ray emission from the core (c) and a signal of HXR monitor.

FIG. 10. Comparison of the parameters of the T-15MD shots discussed in the paper with the boundaries of the working area by density.

## 4.4. Analysis of the first wall materials

Investigation of the plasma-wall interaction is one of the objectives of the T-15MD research program [2]. In the first experiments, the plasma facing components (PFC) were presented by non-magnetic austenitic steel (VV walls and EC launch mirrors) and graphite (protective tiles on the first wall, divertor elements, and limiters) [4]. The presence of graphite elements inside the VV leads to the formation of amorphous hydrocarbon films (a-C:H films), which occurs during both the plasma discharges and the wall conditioning process due to transport and redeposition of products of carbon erosion (atomic carbons and hydrocarbon radicals). To study the processes of carbon erosion and redeposition, as well as the properties of a-C:H films, collecting probes were installed in the T-15MD VV in different toroidal cross-sections of the tokamak. They were located on the high- and low-field sides, in the equatorial plane, and in the upper and lower divertor regions. Substrates made of single-crystal silicon, tungsten, and stainless steel were used as probes. The collecting probes were installed inside of the T-15MD VV immediately before the start of the evacuation of the facility and were removed at the end of the experimental campaign. Protective shutters and sample handling devices were not used, so the surface morphology, as well as the thickness of the a-C:H films, represented a superposition of the effects of working and cleaning discharges.

Visual analysis of the sample surfaces after their removal revealed the presence of films, primarily located on shaded surfaces (Fig. 11). The facilities and equipment of the resource centers of NRC "Kurchatov Institute" are actively used for the comprehensive studies of materials exposed to plasma. The elemental and phase

composition of samples at the nanoscale, the surface morphology of nanostructures formed as a result of plasma interaction with the PFC have been investigated.



FIG. 11. The plasma-facing surface of a silicon sample. The location of a-C:H film deposition, which was in the shadow of the holder's fastening element, is shown by the dashed line.

The composition of a-C:H films was studied using energy-dispersive X-ray spectroscopy (EDRS). Analysis revealed that despite the presence of plasma-facing stainless steel elements on the first wall, located on the LFS, the total Fe, Ni, and Cr content in the studied films is negligible compared to the carbon content (<0.75% in samples mounted on the LFS and <1.8% on the HFS). Thus, the sequential action of working and cleaning

discharges leads to carbonization of the entire inner surface of the VV, and, consequently, to a significant reduction in the formation of heavy impurities. The features of the electronic structure of thin (2-5 nm) carbon films were revealed using X-ray photoelectron spectroscopy (XPS). Tungsten and silicon carbides (1.2-5.6 and 0.8 at.%, respectively) were detected in the C1s, W4f, and Si2p spectra [25] at the film-substrate interface of W and Si. Such phases were not detected in previous studies neither on the T-10 tokamak with graphite limiters, no in the high-current plasma accelerator QSPA-T [26]. Analysis of a-C:H films deposited on the collecting probes revealed a strong poloidal asymmetry in the deposition of eroded carbon. Minimal carbon concentration (~2-8 at.%) corresponding to the film thickness of 2-10 nm is observed on the HFS and in the bottom of VV. These areas are zones of predominant carbon erosion, which is associated with the small distance between the surface of the graphite tiles and the plasma boundary, as well as the direct contact of the hot plasma with the first wall. A zone of predominant a-C:H films deposition was observed on LFS: the carbon concentration on the samples ~ 60-80 at.%, corresponding to the film thickness exceeding 100 nm.

#### 5. SUMMARY

The T-15MD facility began operation in the spring of 2023. Discharges with plasma currents up to 0.6 MA were achieved during several experimental campaigns.

Stable discharges with an elongation of k up to 1.7 and a duration exceeding 2 seconds were obtained in limiter and divertor configurations. Density and temperature profiles of the obtained regimes correspond to the L-mode. Energy confinement time was found to be in a satisfactory agreement with ITER L-89P scaling law.

T-15MD experiments were carried out with ECR assisted start-up. EC power was varied in the range of  $P_{EC}$  = 0.47-1 MW. In all cases, ECR initiated breakdown occurred in the  $2\omega_{ce}$  resonance region. Discharges with  $E_{\parallel}$  < 0.3 V/m throughout the discharge duration were obtained.

In the nearest future, work at the T-15MD facility will be focused at the development of a discharge scenario, increase of the EC heating power up to 5 MW, commissioning of the first neutral beam injector, and expanding the range of physical research.

## **ACKNOWLEDGEMENTS**

The work was supported by the National Research Center "Kurchatov Institute" under the State Assignment.

## REFERENCES

- [1] SMIRNOV, V.P., Tokamak foundation in USSR/Russia 1950-1990, Nuclear Fusion 50 1 (2010) 014003.
- [2] VELIKHOV, E.P., KOVALCHUK, M.V., ANASHKIN, I.O., et al., Physical research program on the T-15MD tokamak, Problems of atomic science and technology, ser. «Thermonuclear fusion» **47** 4 (2024) 9-183 (in Russian).
- [3] VELIKHOV, E.P., KOVALCHUK, M.V., ANASHKIN, I.O. et al., First Experimental Results on the T-15MD Tokamak, Phys. of atomic nucl. 87 1 (2024) S1-S9.
- [4] KHVOSTENKO, P.P., ANASHKIN, I.O., BONDARCHUK, E.N.,et al., Experimental thermonuclear installation Tokamak T-15MD, Phys. of atomic nucl. **83** 7 (2020) 1037-1057.

- [5] ANASHKIN, I.O., KOCHIN, V.A., OBRAZTSOV, I.S., Pumping system of the vacuum chamber of the tokamak T-15MD unit, Phys. of atomic nucl. **87** 7 (2024) 876-883.
- [6] PIMENOV, I.S., BORSCHEGOVSKIY, A.A., AKHMEDOV, E.R., et al, The first test results of the gyrotron and waveguide path of the T-15MD tokamak in a long-pulse operation, Plasma Phys. Reports, **50** 12 (2024) 1594-1598.
- [7] KIRNEVA, N.A., BORSHCHEGOVSKII, A.A., KUYANOV, A.Yu., PIMENOV I.S., ROI I.N., Possibility of using the 140 GHz frequency for ECR plasma heating in the T-15MD tokamak, Phys. of At. Nuclei, **85** 7 (2022) 1181.
- [8] IZAROVA, A.D., BELOV, A.M., ELISEEV, L.G., et al., Methods for Processing signals of magnetic probes at the T-15MD tokamak, Plasma Physics Reports **51** 4 (2025) 397-413.
- [9] ASADULIN, G.M., BEL'BAS, I.S., GORSHKOV, A.V., et al., Thomson scattering diagnostics with tangential probing geometry at the T-15MD Tokamak, Plasma Phys. Rep. **50** (2024) 1327–1336
- [10] DROZD, A.S., SERGEEV, D.S., BEGISHEV, R.A., et al., T-15MD Tokamak microwave interferometer for measuring the average electron density of plasma, Plasma Physics Reports, 50 5 (2024) 568–572.
- [11] SARANCHA, G.A., DROZD, A.S., KUDASHEV, M.S., SERGEEV, D.S., Fiber optic current sensors concept for the T-15MD tokamak, Phys. of atomic nucl. **88** S1 (2025) S21-S28.
- [12] MELNIKOV A.V., SUSHKOV A.V., BELOV A.M., et al, Physical Program and Conceptual Design of the Diagnostics of the T-15 Upgrade Tokamak, Fusion Engineering and Design 96–97 (2015) 306–310.
- [13] MELNIKOV A.V., KRUPNIK L.I., ELISEEV L.G., et al, Heavy ion beam probing diagnostics to study potential and turbulence in toroidal plasmas. Nucl. Fusion 57 (2017) 072004.
- [14] MARTYN, Y.R., TAKIZUKA, T., ITPA CDBM H-mode Threshold Database Working Group, Power Requirement for Accessing the H-mode in ITER, J.Phys.Conf. Ser. **123** (2008) 012033.
- [15] DOYLE, E.J., HOULBERG, W.A., KAMADA, Y., Chapter 2: Plasma confinement and transport, Nucl.Fus. 47 6 (2007) S18-S127.
- [16] BIRKENMEIER, G., SOLANO E.R., CARVALHO I.S., et al., The role of the isotope mass and transport for H-mode access in tritium containing plasmas at JET with ITER-like wall, Plasma Phys. Control. Fusion, **65** 5 (2023) 054001.
- [17] KORENEV, P.S., KONKOV, A.E., MITRISHKIN, Y.V., et al, Improved FCDI algorithm for tokamak plasma equilibrium reconstruction, Technical Physics Letters 49 7 (2023) 34-37.
- [18] ULASEVICH, D.L., ANDREEV, V.F., LUKASH, V.E., KHAYRUTDINOV, R.R., Study of the accuracy of plasma boundary reconstruction in the T-15MD tokamak using the D\_BOUND code", Submitted to Plasma Phys. Reports, 2025.
- [19] YUSHMANOV, P.N., TAKIZUKA, T., RIEDEL, K.S., et al, Scalings for tokamak energy confinement, Nucl. Fusion **30** 10 (1990) 1999.
- [20] KURSKIEV, G.S., GUSEV, V.K., SAKHAROV N.V., et al., Energy confinement in the spherical tokamak Globus-M2 with a toroidal magnetic field reaching 0.8 T, Nucl. Fusion **62** 1 (2022) 016011.
- [21] ZVONKOV, A.V., KUYANOV, A.YU., SKOVORODA, A.A., TIMOFEEV, A.V., ECR current drive in the autoresonance regime in closed confinement systems, Plasma Phys. Rep. **24** 5 (1998) 389-400.
- [22] DNESTROVSKIY, Y.N., NEUDACHIN, S.V., PEREVERSEV, G.V., Simulation of particle balance in a tokamak, Sov. J. of Pl. Phys., 10 2 (1984) 236-244
- [23] SYCHUGOV, D.YU., RYZHAKOV, D.V., ANDREEV, V.F., et al., Modelling of stable equilibrium magnetic configurations for the first experiments on the tokamak T-15MD, Phys. of atomic nucl. **88** 1 (2025) S1-S12.
- [24] de VRIES, P.C., MINEEV, A.B., GRIBOV, Y., et al, Comparison of start-up runaway electron generation simulations using the SCENPLINT code with JET experimental observations, Nucl. Fusion **65** 5 (2025) 056001.
- [25] ARKHIPOV, I.I., GRASHIN, S.A., KAPUSTIN, YU.V., SVECHNIKOV, N.YU., CHUMAKOV, R.G., LUKASHEVICH, A.V., "Erosion and redeposition of carbon in the T-15MD tokamak during operating and cleaning discharges", to be published in Proc. of XXI All-Russian Conference "HIGH-TEMPERATURE PLASMA DIAGNOSTICS", 2025.
- [26] STANKEVICH, V.G., SVECHNIKOV, N.Y., KOLBASOV, B.N., Comparative analysis of spectroscopic studies in tungsten and carbon deposits on plasma-facing components in thermonuclear fusion reactors, Symmetry, **15** 3 (2023) 623.